catalysts

MDPI

Article

Design and Characterization of a Novel Artificial Peroxidase

Ye Yuan [1], Jia Xu [1], Zhenyu Zhao [1], Hui Li [1], Kai Wang [1], Zhi Wang [1,2,3,*] and Liping Wang [1,2,3,*]

1 School of Life Sciences, Jilin University, Changchun 130012, China; yeyuan18@mails.jlu.edu.cn (Y.Y.); xujia16@mails.jlu.edu.cn (J.X.); zhenyu18@mails.jlu.edu.cn (Z.Z.); lihui18@mails.jlu.edu.cn (H.L.); wangkai17@mails.jlu.edu.cn (K.W.)
2 Key Laboratory for Molecular Enzymology and Engineering, the Ministry of Education, Jilin University, Changchun 130012, China
3 Engineering Laboratory for AIDS Vaccine, Jilin University, Changchun 130012, China
* Correspondence: wangzhi@jlu.edu.cn (Z.W.); wanglp@jlu.edu.cn (L.W.); Tel.: +86-431-8518-2281 (Z.W.); +86-431-8515-5348 (L.W.)

Received: 18 January 2019; Accepted: 7 February 2019; Published: 11 February 2019

Abstract: In this study, we reported on a novel mimetic peroxidase, deuterohemin–Ala–His–Glu, (Dh–A–H–E). The kinetic parameters of Dh–A–H–E suggested that it was a mimetic peroxidase and followed the ping–pong mechanism. Compared to horseradish peroxidase, Dh–A–H–E exhibited excellent stability when tested at different pH and temperatures, and using different organic solvents. Based on our above results, a new method using Dh–A–H–E has successfully been developed for the fast and quantitative detection of trace amounts of glucose.

Keywords: Dh–A–H–E; mimetic peroxidase; kinetics; catalytic activity; stability; glucose detection

1. Introduction

Horseradish peroxidase (HRP) is a naturally occurring enzyme that has been widely applied in organic synthesis and biotransformation [1]. For example, it has been successfully used as a bleaching detergent. It can activate hydrogen peroxide and convert the nonluminescent substrate, 3,3′,5,5′–tetramethylbenzidine (TMB), into a luminescent product, oxidized TMB (oxTMB). This application of HRP has been used for analytical diagnostics [2,3]. Furthermore, HRP can be used in many small–scale organic reactions, including oxidative coupling [4], selective hydroxylation [5], and oxygen–transfer reactions [6]. However, high temperatures, harsh pH conditions, and a number of chemical compounds can denature HRP easily, which severely limits its extensive application [7–9]. Owing to the limitations on reaction conditions, many efforts have been made to find, or design, a new artificial enzyme to mimic HRP. In the past decades, many small molecule analogs (fluorescein [10], ferrocene [11], etc.), and nanomaterials (Au nanoclusters [12], cobalt incorporated mesoporous silica nanomaterials [13], etc.) have been reported to have peroxidase–like activity. However, the majority of these reported enzyme mimics possess only poor peroxidase activity.

As a kind of peroxidase mimic, Heme–peptide has been researched for years because it is highly stable and can be easily synthesized. Heme–peptides are produced by covalently linking peptides to ferriporphyrin and have shown great potential for use in medical detection, as biocatalysts, sensitive sensors, and in other applications [14–16]. Microperoxidases (MPs) have been the most effective peroxidases among these heme–peptides. Several MPs have been previously characterized, such as microperoxidase–11 (MP–11), microperoxidase–9 (MP–9), and microperoxidase–8 (MP–8). Owing to their high peroxidase activity, external stability, and structural consistency, MPs have been used in many applications. However, the chemical synthesis of MP–11 has proven difficult [17].

We chemically synthesized the catalytically active center, comprising of deuterohemin (Dh) linked to alanine and histidine, according to a published method [18,19]. When glutamic acid (E) was linked to the catalytically active center to generate Dh–A–H–E, it was found that this new heme–peptide could efficiently catalyze TMB in the presence of H_2O_2 (Scheme 1). In addition, the catalytic properties of Dh–A–H–E were investigated. Another important advantage of Dh–A–H–E is that its optimal pH is 7.4 and it can exhibit high peroxidase activity at pH 7.0, which can dramatically simplify the procedure of glucose detection [20–22]. Thus, an improved method for detecting trace amounts of glucose using Dh–A–H–E was developed.

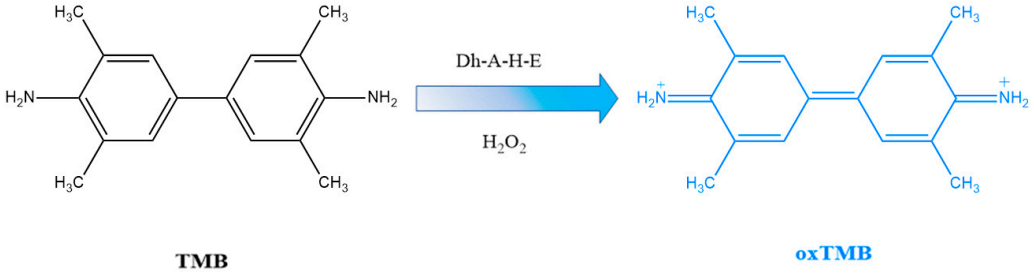

Scheme 1. Catalytic reaction of deuterohemin–Ala–His–Glu (Dh–A–H–E).

2. Results and Discussion

2.1. The Peroxidase Activity of Deuterohemin–Ala–His–Glu (Dh–A–H–E)

To evaluate the catalytic activity of Dh–A–H–E as a mimetic peroxidase, TMB was mixed with Dh–A–H–E in the presence of H_2O_2. As shown in Figure 1, solutions containing TMB and low concentrations of Dh–A–H–E were almost colorless, while the solution of TMB and H_2O_2 was slightly blue. When we mixed Dh–A–H–E, TMB, and H_2O_2 together for 5 min, a blue solution was obtained, and a strong characteristic absorption peak of oxidized TMB (oxTMB) was observed at 652 nm. These results indicated that Dh–A–H–E had peroxidase activity.

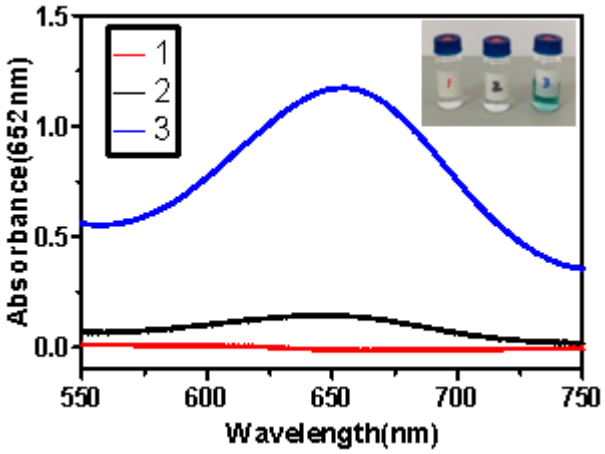

Figure 1. UV absorption of (**1**) Dh–A–H–E + 3,3′,5,5′–tetramethylbenzidine (TMB), (**2**) TMB + H_2O_2, and (**3**) Dh–A–H–E + TMB + H_2O_2.

2.2. Optimizing the Reaction Conditions

Temperature and pH can influence the catalytic activity of peroxidases, including HRP and other peroxidase mimics [23,24]. Thus, to determine the optimal reaction conditions for the peroxidase activity of Dh–A–H–E, we tested a variety of experimental conditions. The relationship between the temperature and catalytic activity of Dh–A–H–E is shown in Figure 2a, with the optimal temperature for Dh–A–H–E activity occurring at 25 °C. The optimal pH for Dh–A–H–E catalytic activity was 7.4 and the effect of pH on activity is shown in Figure 2b.

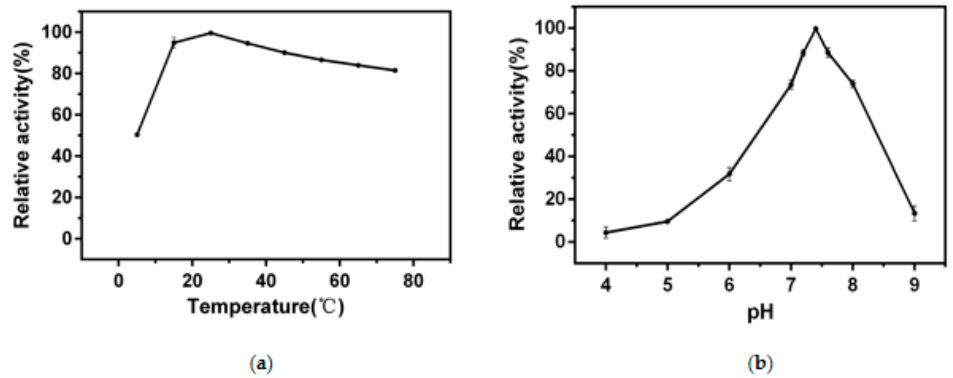

Figure 2. Effect of temperature and pH on the catalytic activity of Dh–A–H–E. (**a**) The reaction was carried out at different temperatures (5–75 °C) and the peroxidase activity of Dh–A–H–E was measured according to the standard assay in Section 3.3. (**b**) The reaction was carried out under various pH levels (4–9) and the peroxidase activity of Dh–A–H–E was measured according to the standard assay in Section 3.3. The catalytic activity at pH 7.4 and 25 °C is taken as 100%, and experiments were performed in triplicate to obtain the mean value.

2.3. Kinetics

To further characterize the catalytic ability of Dh–A–H–E, the reaction rates under different conditions were measured across various substrate concentrations corresponding to the Michaelis–Menten curves for both H_2O_2 (Figure 3a) and TMB (Figure 3b). Double–reciprocal plots were generated to analyze the kinetic parameters with H_2O_2 and TMB (Figure 3c,d). From Table 1, the K*m* (the Michaelis constant, representing the affinity of the enzyme for the substrate) of Dh–A–H–E was calculated to be 0.27 mM for H_2O_2 and 0.20 mM for TMB. The K*cat* (the turn number) of Dh–A–H–E was calculated to be 2.37 s^{-1} for H_2O_2 and 2.10 s^{-1} for TMB. The catalytic efficiency (K*cat*/K*m*) of Dh–A–H–E was measured to be 8.78 × 10^2 s^{-1}·M^{-1} for H_2O_2 and 1.05 × 10^3 s^{-1}·M^{-1} for TMB. These data indicated that Dh–A–H–E had both a high affinity and a high catalytic activity.

Table 1. The catalytic efficiency of Dh–A–H–E.

Catalyst	Substrate (TMB)			Substrate (H_2O_2)		
	K*m* (mM)	K*cat* (s^{-1})	K*cat*/K*m* (s^{-1}·M^{-1})	K*m* (mM)	K*cat* (s^{-1})	K*cat*/K*m* (s^{-1}·M^{-1})
Dh–A–H–E	0.20	2.10	1.05 × 10^3	0.27	2.37	8.78 × 10^2

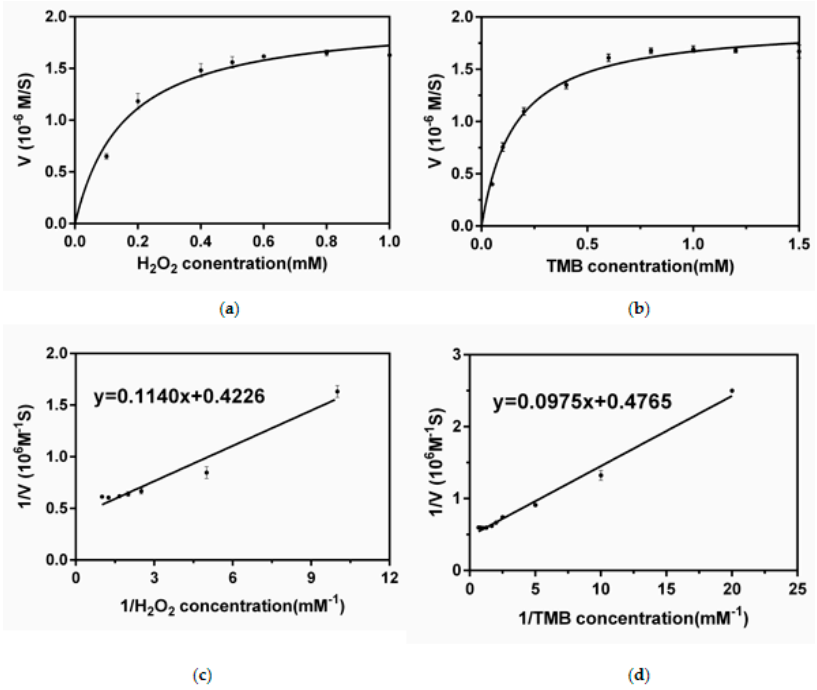

Figure 3. Kinetics assay of Dh–A–H–E. (**a**) Michaelis–Menten curves against H_2O_2 concentration, in which the concentration of TMB was fixed at 2.0 mM; (**b**) Michaelis–Menten curves against TMB concentration, in which the concentration of H_2O_2 was fixed at 1.0 mM; (**c**) double–reciprocal curves against H_2O_2, in which the concentration of TMB was fixed at 2.0 mM; and (**d**) double–reciprocal curves against TMB, in which the concentration of H_2O_2 was fixed at 1.0 mM. Experiments were performed in triplicate to obtain the mean value.

2.4. Catalytic Mechanism

Analysis of the reaction mechanism was conducted by varying the concentrations of H_2O_2 and TMB (Figure 4a,b). A set of fixed TMB concentrations was chosen, and the concentration of H_2O_2 was varied at each TMB concentration. The data were plotted in double–reciprocal form, which provided a series of apparently parallel lines. A series of parallel lines could also be observed by re–plotting the data with TMB as the variable substrate. Just like the natural HRP [25], the linearity of the double–reciprocal plots for both the H_2O_2 and TMB preparations strongly supported a ping–pong mechanism.

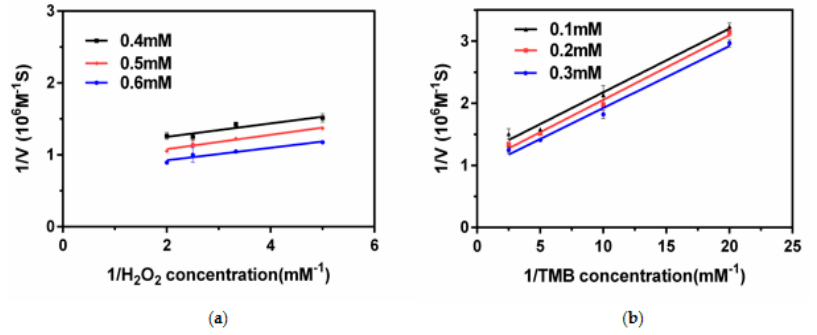

Figure 4. (**a**) Double–reciprocal plots at different H_2O_2 concentrations, in which the concentration of TMB was fixed at 0.4, 0.5, and 0.6 mM; (**b**) double–reciprocal plots at different TMB concentrations, in which the concentration of H_2O_2 was fixed at 0.1, 0.2, and 0.3 mM. Experiments were performed in triplicate to obtain the mean value.

2.5. Stability of Dh–A–H–E

The stability of Dh–A–H–E is crucial for extending its potential applications. In this study, Dh–A–H–E was pre–incubated for 2 h at different pH and temperatures, and using different organic solvents. Then, we examined the residual activity of Dh–A–H–E to evaluate its stability. Dh–A–H–E retained over 70% of its activity following a 2 h incubation at pH 4.4–9.4 for 2 h, as shown in Figure 5a. After a 2 h incubation at different temperatures, Dh–A–H–E retained >95% of its baseline activity (Figure 5b). The residual activity of Dh–A–H–E after a 2 h incubation with organic solvents (DMSO, acetone, and acetonitrile) was >38% of the baseline activity (Figure 5c). By contrast, HRP had little catalytic activity in organic solvents or at high temperatures [26]. Another important advantage of Dh–A–H–E is that it retains its catalytic activity even after storage in an aqueous solution for 3 months (Figure 5d). These results demonstrated that Dh–A–H–E had excellent stability and was very suitable for real–life applications.

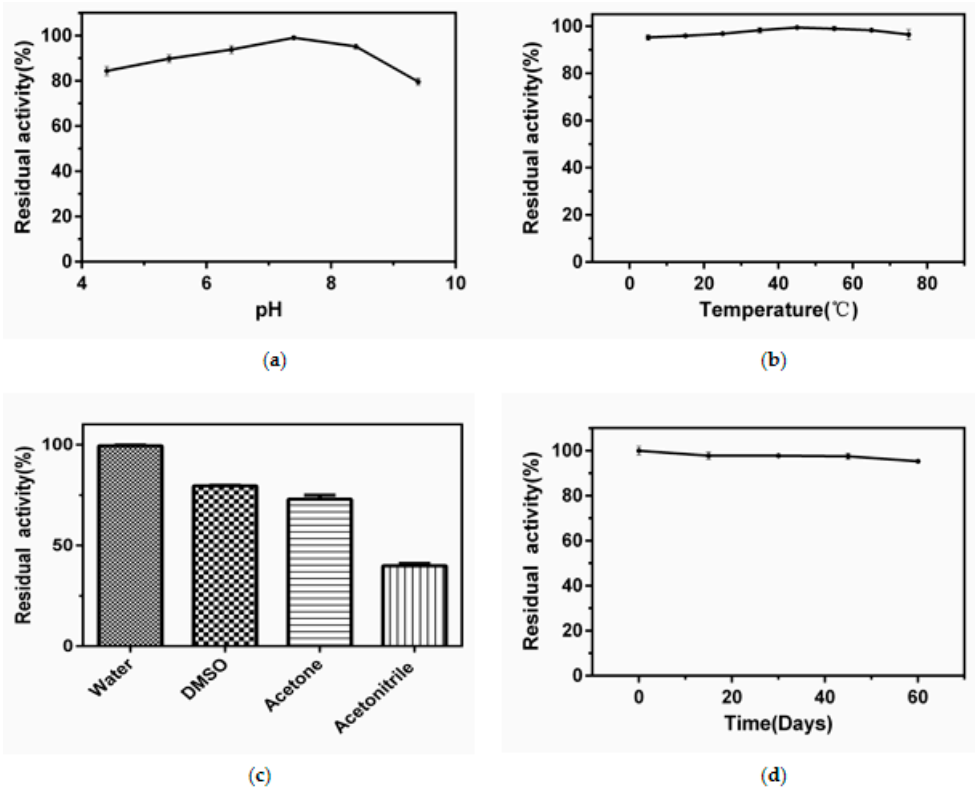

Figure 5. Stability of Dh–A–H–E. (**a**) Dh–A–H–E was incubated at a range of pH values from 4.4 to 9.4 for 2 h, and then the residual activity was measured according to the standard assay in Section 3.3; (**b**) Dh–A–H–E was incubated at a range of temperature values from 5 to 75 °C for 2 h, and then the residual activity was measured according to the standard assay in Section 3.3; (**c**) Dh–A–H–E was incubated with different organic solvents (DMSO, acetone, and acetonitrile), and then the residual activity was measured according to the standard assay in Section 3.3; and (**d**) Dh–A–H–E was stored in an aqueous solution for a certain number of days, then the residual activity was measured according to the standard assay in Section 3.3. Experiments were performed in triplicate to obtain the mean value.

2.6. Application of Dh–A–H–E for H_2O_2 and Glucose Detection

On the basis of the above results, we developed a sensitive and simple system for detecting the trace amounts of H_2O_2 glucose by Dh–A–H–E (Figure 6a). A good linear relationship between the absorbance at 652 nm and the concentration of H_2O_2 can be observed in Figure 6a. The detection limit was in the range of 2.0–75 μM, and the linear regression equation was A = 0.0160C + 0.0706 (R^2 = 0.9820). The detection limit was 0.5 μM. Compared to other peroxidases [27–30] (Table S1),

the excellent sensitivity of Dh–A–H–E makes it well–suited for H_2O_2–mediated glucose detection. First, glucose was oxidized by glucose oxidase (GO_x) in NaH_2PO_4–Na_2HPO_4 buffer (pH 7.0) for 30 min to produce H_2O_2. Then, Dh–A–H–E and TMB were directly added to this solution for another 5 min. A typical glucose concentration–response curve was obtained and plotted in Figure 6b, with a linear regression equation of A = 0.0073C + 0.2553 (R^2 = 0.9601). The linear range of glucose detection for the assay was between 10 μM and 0.18 mM, with a detection limit of 2 μM. These parameters were more sensitive than other similar peroxidase mimic–based methods, as in [27–30] (detailed in Table S2).

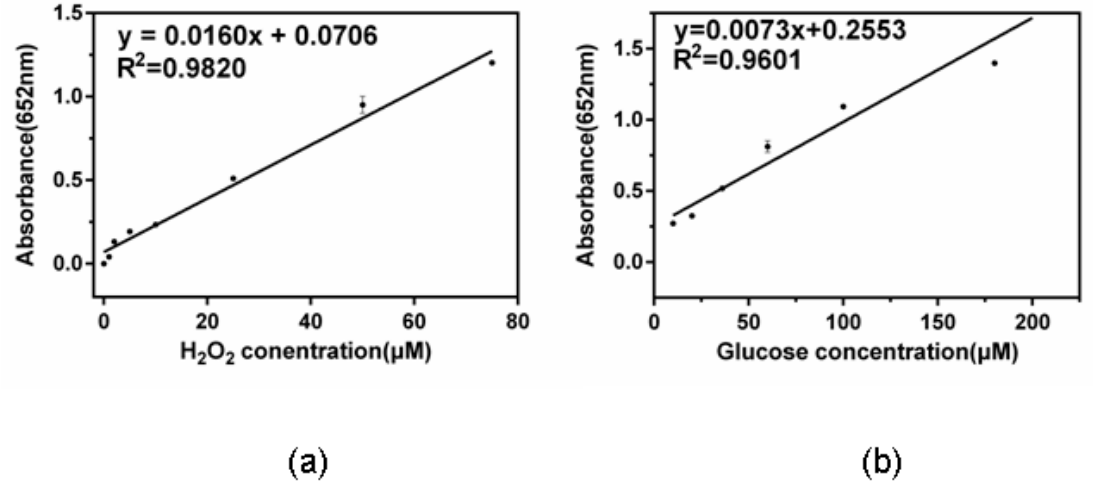

Figure 6. (**a**) Linear regression plot against different concentrations of H_2O_2; (**b**) linear regression plot against different concentrations of glucose. Experiments were performed in triplicate to obtain the mean value.

3. Materials and Methods

3.1. Materials

Rink amide resin, Fmoc amino acids, 1–hydroxybenzotriazole (HOBT), and benzotriazol–1–yl–oxytripyrrolidinophosphonium hexafluorophosphate (PYBOP) were purchased from Gl Biochem (Shanghai, China). *N*,*N*–Dimethylformamide (DMF) and dichloromethane (DCM) were purchased from Beijing Beihua Fine Chemicals Co., Ltd. (Beijing, China). Acetonitrile (HPLC grade, ≥99%) was purchased from Oceanpak Alexative Chemicals Co., Ltd. (Gothenburg, Sweden). TMB, H_2O_2 (30%), and glucose oxidase (GO_x, 200 U/mg) were purchased from Dalian Meilun Biotechnology Co., Ltd. (Dalian, China). Ultrapure water was prepared using an ultrapure water purification system (Sichuan, China).

3.2. Synthesis of Dh–A–H–E

Dh–A–H–E was synthesized using solid phase peptide synthesis technology. The reaction was carried out in a solid phase peptide reactor. Rink amide resin was swelled in the reactor for 1 h with DCM. The deprotection reagent was then added to the reactor in DMF. Then, a three–fold excess of the Fmoc group–protected amino acids, HOBT and PYBOP, and a six–fold excess of organic base were added to the reactor in DMF for 2 h. Then, deuterohemin/HOBT/PYBOP/organic base/rink amide resin were added in the amount of substance ratio 0.8:1.5:1.2:2:1 to the reactor, in DCM, for at least 8 h. The peptide was dried in a vacuum dryer. Trifluoroacetic acid was used to cleave the peptide from the resin. The crude peptide was purified by Reversed–phase high–performance liquid chromatography (RP–HPLC). Dh–A–H–E was analyzed by RP–HPLC at 387 nm (Figure S1) and identified by Time–of–flight mass spectrometry (TOF–MS) (Figure S2). The synthesized peptide, with a purity of more than 95%, was obtained.

3.3. Standard Peroxidase Activity Assay of Dh–A–H–E

The reaction was carried out in a 1 mL cuvette. NaH_2PO_4–Na_2HPO_4 buffer solution (0.7 mL, 0.1 M, pH 7.4), TMB (0.1 mL, 10 mM), Dh–A–H–E (0.1 mL, 10 μM), and H_2O_2 (0.1 mL, 5 mM) were added in order. The reaction was carried out at 25 °C for 5 min. The oxidation product of TMB was detected with a UV–VIS recording spectrophotometer (UV–2501PC) at 652 nm. Experiments were performed in triplicate to obtain the mean value.

3.4. Optimizing the Reaction Conditions

To investigate the effect of temperature, the reaction was carried out at different temperatures (5, 15, 25, 35, 45, 55, 65, and 75 °C). Then, the peroxidase activity assay of Dh–A–H–E was measured according to the standard assay in Section 3.3.

To investigate the effect of pH, the reaction was carried out at different pH l (4, 5, 6, 7, 7.2, 7.4, 7.6, 8 and 9). Then, the peroxidase activity assay of Dh–A–H–E was measured according to the standard assay in Section 3.3.

3.5. Kinetics of Dh–A–H–E

The kinetic assays were implemented at 25 °C in 1 mL NaH_2PO_4–Na_2HPO_4 buffer solution (0.1 M, pH 7.4), containing 100μL Dh–A–H–E (10 μM) as a peroxidase in the presence of H_2O_2 and TMB. The kinetic constant of Dh–A–H–E with H_2O_2 as a substrate was obtained by adding a certain concentration (2.0 mM) of TMB and different concentrations (0.1, 0.2, 0.4, 0.5, 0.6, 0.8 and 1.0 mM) of H_2O_2. The kinetic constant of Dh–A–H–E with TMB as a substrate was obtained by adding a certain concentration (1.0 mM) of H_2O_2 and different concentrations (0.05, 0.1, 0.2, 0.4, 0.5, 0.6, 0.8, 1.0, 1.2 and 1.5 mM) of TMB.

3.6. Stability of Dh–A–H–E

The stability was tested in this study. Dh–A–H–E was incubated at different pH (4.4, 5.4, 6.4, 7.4, 8.4, and 9.4), temperatures (5, 15, 25, 35, 45, 55, 65, and 75 °C), and in different organic solvents (DMSO, acetone, and acetonitrile) for 2 h. Then, the residual activity was measured according to the standard assay in Section 3.3.

3.7. Detection of the Trace Concentration of H_2O_2 and Glucose Using Dh–A–H–E

First, glucose oxidase (GO_x, 20 μL, 1.0 mg/mL), 20 μL of glucose at different concentrations, and NaH_2PO_4–Na_2HPO_4 buffer (160 μL, 0.1 M, pH 7.0) were mixed and incubated at 37 °C for 30 min. Then, NaH_2PO_4–Na_2HPO_4 buffer (600 μL, 0.1 M, pH 7.4), TMB (100μL, 10 mM), and Dh–A–H–E (100 μL, 10 μM) were added to the above solution together. The mixture was incubated at 25 °C for 5 min, and the absorbance was recorded at 652 nm.

4. Conclusions

In this study, we reported on the synthesis of a novel mimetic peroxidase, Dh–A–H–E. Dh–A–H–E can be easily synthesized using solid phase peptide synthesis technology. Its high peroxidase activity towards TMB and its excellent stability in a range of harsh environmental conditions indicates that Dh–A–H–E is a valid mimetic peroxidase, and that its properties make it ideal in industrial and medical testing applications.

Supplementary Materials: The following are available online at http://www.mdpi.com/2073-4344/9/2/168/s1. Figure S1: RP–HPLC of Dh–A–H–E; Figure S2: TOF–MS of Dh–A–H–E; Table S1: Comparison of the various mimetic peroxidases for H_2O_2 detection; Table S2: Comparison of various mimetic peroxidases for glucose detection.

Author Contributions: Conceptualization, L.W. and Z.W.; methodology, Y.Y.; software, Y.Y.; J.X., and Z.Z.; validation, J.X., Y.Y. and Z.Z.; formal analysis, H.L., K.W. and Y.Y.; investigation, Y.Y.; resources, Z.Z.; data curation, Y.Y.; writing—original draft preparation, Y.Y.; writing—review and editing, Z.W. and L.W.

Funding: This research was funded by the Special Project for Health from Jilin Province (No. 2018SCZWSZX–037).

Conflicts of Interest: The authors declare no conflict of interest.

References

1. Veitch, N.C. Horseradish peroxidase: A modern view of a classic enzyme. *Phytochemistry* **2004**, *65*, 249–259. [CrossRef]
2. Sun, H.; Jiao, X.; Han, Y.; Jiang, Z.; Chen, D. Synthesis of Fe_3O_4–Au nanocomposites with enhanced peroxidase–like activity. *Eur. J. Inorg. Chem.* **2013**, *1*, 109–114. [CrossRef]
3. Wang, M.; Bao, W.; Wang, J. A green approach to the synthesis of novel "Desert rose stone"—Like nanobiocatalytic system with excellent enzyme activity and stability. *Sci. Rep.* **2014**, *4*, 6606. [CrossRef] [PubMed]
4. Matsumoto, K.; Takahashi, H.; Miyake, Y. Convenient synthesis of neurotrophic americanol A and isoamericanol A by HRP catalyzed oxidative coupling of caffeic acid. *Tetrahedron Lett.* **1999**, *40*, 3185–3186. [CrossRef]
5. Lin, Y.; Liang, M.; Lin, Y. Specifically and reversibly immobilizing proteins/enzymes to nitriolotriacetic–acid–modified mesoporous silicas through histidine tags for purification or catalysis. *Chem. Eur. J.* **2011**, *17*, 13059–13067. [CrossRef] [PubMed]
6. Kobayashi, S.; Nakano, M.; Kimura, T. On the mechanism of the peroxidase–catalyzed oxygen–transfer reaction. *Biochemistry* **1987**, *26*, 5019–5022. [CrossRef] [PubMed]
7. Mu, J.; Zhang, L.; Zhao, M.; Wang, Y. Co_3O_4 nanoparticles as an efficient catalase mimic: Properties, mechanism and its electrocatalytic sensing application for hydrogen peroxide. *J. Mol. Catal. A Chem.* **2013**, *378*, 30–37. [CrossRef]
8. Liu, Y.; Liu, X.; Guo, Z.; Hu, Z.; Xue, Z.; Lu, X. Horseradish peroxidase supported on porous graphene as a novel sensing platform for detection of hydrogen peroxide in living cells sensitively. *Biosens. Bioelectron.* **2017**, *87*, 101–107. [CrossRef] [PubMed]
9. Yang, Y.; Shen, D.; Long, Y.; Xie, Z.; Zheng, H. Intrinsic of peroxidase–like activity of ficin. *Sci. Rep.* **2017**, *7*, 43141. [CrossRef]
10. Liu, L.; Shi, Y.; Yang, Y.; Li, M.; Long, Y.; Huang, Y.; Zheng, H. Fluorescein as an artificial enzyme to mimic peroxidase. *Chem. Commun.* **2016**, *52*, 13912–13915. [CrossRef]
11. Wang, Q.; Ma, K.; Yu, Z.; Ding, J.; Hu, Q.; Liu, Q.; Sun, H.; Wen, D.; Liu, Q.; Kong, J. The peroxidase–like catalytic activity of ferrocene and its application in the biomimetic synthesis of microsphere polyaniline. *New J. Chem.* **2018**, *42*, 13536–13540. [CrossRef]
12. Xia, X.; Long, Y.; Wang, J. Glucose oxidase–functionalized fluorescent gold nanoclusters as probes for glucose. *Anal. Chim. Acta* **2013**, *772*, 81–86. [CrossRef] [PubMed]
13. Ghavidel Hajiagha, N.; Mahmoudi, A.; Sazegar, M.R.; Pouramini, M.M. Synthesis of cobalt–modified MSN as a model enzyme: Evaluation of the peroxidatic performance. *Microporous Mesoporous Mater.* **2019**, *274*, 43–53. [CrossRef]
14. Kalaivani, G.; Sivanesan, A.; Kannan, A.; Sevvel, R. Generating monomeric 5–coordinated microperoxidase–11 using carboxylic acid functionalized silver nanoparticles: A surface–enhanced resonance Raman scattering analysis. *Colloids Surf. B* **2016**, *146*, 722–730. [CrossRef] [PubMed]
15. Lin, Y.W. The broad diversity of heme–protein cross–links: An overview. *Biochim. Biophys. Acta* **2015**, *1584*, 844–859. [CrossRef] [PubMed]
16. Ascenzi, P.; Leboffe, L.; Santucci, R.; Coletta, M. Ferric microperoxidase–11 catalyzes peroxynitrite isomerization. *J. Inorg. Biochem.* **2015**, *144*, 56–61. [CrossRef]
17. Guan, S.; Li, P.; Luo, J. A deuterohemin peptide extends lifespan and increases stress resistance in Caenorhabditis elegans. *Free Radic. Res.* **2010**, *44*, 813–820. [CrossRef]

18. Casella, L.; Gullotti, M.; Monzani, E. Biomimetic oxidation catalysis by iron (III) deuteroporpbyrin carrying a deca–L–alanine peptide chain. *Rend. Lincei* **1991**, *2*, 201–212. [CrossRef]
19. Casella, L.; Monzani, E.; Fantucci, P. Axial imidazole distortion effects on the catalytic and binding properties of chelated deuterohemin complexes. *Inorg. Chem.* **1996**, *35*, 439–444. [CrossRef]
20. Guo, J.; Wang, Y.; Zhao, M. 3D flower–like ferrous(II) phosphate nanostructures as peroxidase mimetics for sensitive colorimetric detection of hydrogen peroxide and glucose at nanomolar level. *Talanta* **2018**, *182*, 230–240. [CrossRef]
21. Pang, Y.; Huang, Z.; Yang, Y.; Long, Y.; Zheng, H. Colorimetric detection of glucose based on ficin with peroxidase–like activity. *Spectrochim. Acta Part A* **2018**, *189*, 510–515. [CrossRef] [PubMed]
22. Zhang, Y.; Zhou, Z.; Wen, F.; Tan, J.; Peng, T.; Luo, B.; Wang, H.; Yin, S. A flower–like MoS_2–decorated $MgFe_2O_4$ nanocomposite: Mimicking peroxidase and colorimetric detection of H_2O_2 and glucose. *Sens. Actuators B* **2018**, *275*, 155–162. [CrossRef]
23. Gao, Y.; Wu, K.; Li, H.; Chen, W.; Fu, M.; Yue, K.; Zhu, X.; Liu, Q. Glutathione detection based on peroxidase–like activity of Co_3O_4–Montmorillonite nanocomposites. *Sens. Actuators B* **2018**, *273*, 1635–1639. [CrossRef]
24. Shi, Y.; Liu, L.; Yu, Y.; Long, Y.; Zheng, H. Acidic amino acids: A new–type of enzyme mimics with application to biosensing and evaluating of antioxidant behavior. *Spectrochim. Acta Part A* **2018**, *201*, 367–375. [CrossRef]
25. Savic, S.; Vojinovic, K.; Milenkovic, S.; Smelcerovic, A.; Lamshoeft, M.; Petronijevic, Z. Enzymatic oxidation of rutin by horseradish peroxidase: Kinetic mechanism and identification of a dimeric product by LC–Orbitrap mass spectrometry. *Food Chem.* **2013**, *141*, 4194–4199. [CrossRef] [PubMed]
26. Li, Y.; Li, T.; Chen, W.; Song, Y. Co_4N Nanowires: Noble–Metal–Free Peroxidase Mimetic with Excellent Salt– and Temperature–Resistant Abilities. *ACS Appl. Mater. Interfaces* **2017**, *9*, 29881–29888. [CrossRef] [PubMed]
27. Jin, L.; Shang, L.; Guo, S.; Fang, Y.; Wen, D.; Wang, L.; Yin, J.; Dong, S. Biomolecule–stabilized Au nanoclusters as a fluorescence probe for sensitive detection of glucose. *Biosens. Bioelectron.* **2011**, *26*, 1965–1969. [CrossRef] [PubMed]
28. Dong, Y.; Zhang, H.; Rahman, Z.U.; Su, L.; Chen, X.; Hu, J.; Chen X., G. Graphene Oxide–Fe_3O_4 Magnetic Nanocomposites with peroxidase–Like Activity for colorimetric detection of glucose. *Nanoscale* **2012**, *4*, 3969–3976. [CrossRef]
29. Li, M.; Liu, L.; Shi, Y.; Yang, Y.; Zheng, H.; Long, Y. Dichlorofluorescein as a peroxidase mimic and its application to glucose detection. *New J. Chem.* **2017**, *41*, 7578–7582. [CrossRef]
30. Malvi, B.; Panda, C.; Dhar, B.B.; Gupta, S.S. One pot glucose detection by [Fe^{III}(biuret–amide)] immobilized on mesoporous silica nanoparticles: An efficient HRP mimic. *Chem. Commun.* **2012**, *48*, 5289–5291. [CrossRef]